Article

Shape-Memory Properties of Segmented Polymers Containing Aramid Hard Segments and Polycaprolactone Soft Segments

Christian Schuh, Kerstin Schuh, Maria C. Lechmann, Louis Garnier and Arno Kraft *

Chemistry, School of Engineering & Physical Sciences, Heriot-Watt University, Edinburgh EH14 4AS, UK; E-Mails: schuh@imtek.de (C.S.); kschuh@imtek.de (K.S.); lechmann@mpip-mainz.mpg.de (M.C.L.); louis_garnier@hotmail.fr (L.G.)

* Author to whom correspondence should be addressed; E-Mail: a.kraft@hw.ac.uk; Tel.: +44-131-4518040; Fax: +44-131-4513180.

Abstract: A series of segmented multiblock copolymers containing aramid hard segments and extended polycaprolactone soft segments (with an M_n of 4,200 or 8,200 g mol^{-1}) was prepared and tested for their shape-memory properties. Chain extenders were essential to raise the hard segment concentration so that an extended rubbery plateau could be observed. Dynamic mechanical thermal analysis provided a useful guide in identifying (i) the presence of a rubbery plateau, (ii) the flow temperature, and (iii) the temperature when samples started to deform irreversibly.

Keywords: shape-memory polymer; aramid; polycaprolactone

1. Introduction

When an elastic material is deformed, elastic energy is stored within the material but is immediately recovered once the applied stress is released [1,2]. In contrast, deformation of a shape-memory material leads to a stable temporary shape. As in the case of an elastomer, elastic energy is stored within the material; however, unlike an elastomer, its release requires the application of an external trigger which is usually heat but can also be a magnetic field or light [3,4]. Shape-memory alloys such as nickel–titanium alloy (Nitinol) are widely studied shape-memory materials, with applications ranging from

flexible spectacle frames to stents and actuated devices. Despite their wide-spread use, shape-memory alloys are comparatively expensive and have limited maximum strain (≤8%). They can, however, support high loads. If only small loads are needed, then shape-memory polymers (SMPs) offer an attractive alternative due to their low manufacture cost and ease of processing. In addition, SMPs can withstand much higher elongations of several hundred percent in some cases. The recently developed two-way and triple-shape SMPs possess even more than one programmed shape [5,6].

Many SMPs are based on a segmented, multiblock copolymer structure [1]. In a large number of cases, these thermoplastic SMPs were polyurethanes containing urethane hard segments and suitably chosen polyether or polyester soft segments [7,8]. The soft segments in SMPs can be either amorphous or semicrystalline. A key design feature of SMPs requires that the soft segment gives rise to a thermal transition slightly above the working temperature. In practice, this means that the soft segment must possess either a melting or a glass transition just above room or body temperature. In this respect SMPs differ from thermoplastic elastomers whose glass transition temperature (T_g) is generally located well below room temperature. One of the more popular soft segments is polycaprolactone (PCL), a semicrystalline polymer with a melting temperature (T_m) between 35 and 55 °C depending on the molecular weight of the soft segment (3,000–8,000 g mol^{-1}) [3,6-8].

In the last decade, Gaymans and co-workers have demonstrated in a series of papers that replacement of urethanes by aramid (aromatic amide) units provides a number of advantages which lead to a significant improvement in mechanical properties over related polyurethane elastomers [9,10]. Uniform aramid hard segments crystallize fast, show excellent phase separation, and give rise to a high fracture strain and toughness. We have reported a synthetic route to segmented multiblock copolymers with aramid hard segments and polytetrahydrofuran or polycarbonate soft segments [11,12], including polymers with polycaprolactone soft segments of intermediate molecular weight (3,000 g mol^{-1}) which showed promising shape-memory properties [13]. This paper discusses the further development of segmented aramid-based SMPs in which we increased the molecular weight of the polycaprolactone soft segments above 4,000 g mol^{-1}. However, extended soft segments necessitated the incorporation of additional hard segments which was achieved by copolymerization with a suitable short-chain telechelic ("chain extender"). Dynamic mechanical thermal analysis (DMTA) served as a useful tool to identify polymers with promising shape-memory properties.

2. Results and Discussion

2.1. Synthesis

All segmented multiblock (co)polymers were synthesized by the reaction of an aminobenzoyl-terminated polycaprolactone (**PCL4200** or **PCL8200**) with terephthaloyl chloride in the presence of chlorotrimethylsilane at room temperature (Scheme 1). The condensation is known to involve an *N,N'*-bis(trimethylsilyl)-substituted aromatic diamine intermediate which is susceptible to hydrolysis, an undesired side reaction that can be prevented by making the silylated intermediate *in situ* [14,15]. A range of copolymers was subsequently made by replacing part of **PCL4200** or **PCL8200** with short-chain telechelics **T1**–**T4** (Scheme 2). These telechelics served as "chain extenders" and, like

the chain extenders in polyurethane chemistry, they were expected to raise the hard segment content and thus the modulus of the copolymer (Scheme 3). They were chosen because of their different segment length (increasing from **T1** to **T3**/**T4**) and their ready availability. We were also interested to determine whether shorter or longer segments within the chain extender would be more beneficial. Details of the composition of the polymers studied in this paper are summarized in Table 1.

Scheme 1. Structure of **PCL4200/PCL8200** and typical polymerization procedure (soft segments are highlighted in blue, hard segments in red).
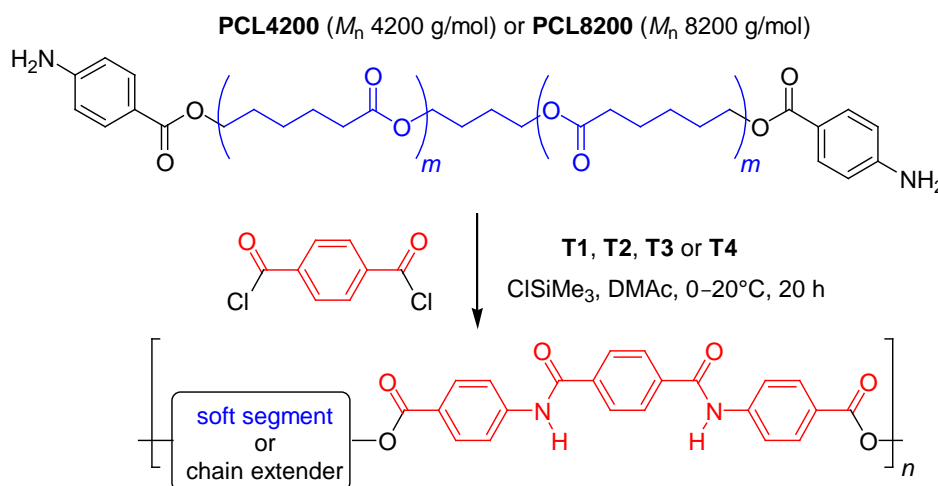
Scheme 2. Structures of short-chain telechelics **T1**–**T4** ("chain extenders") used in copolymerizations.
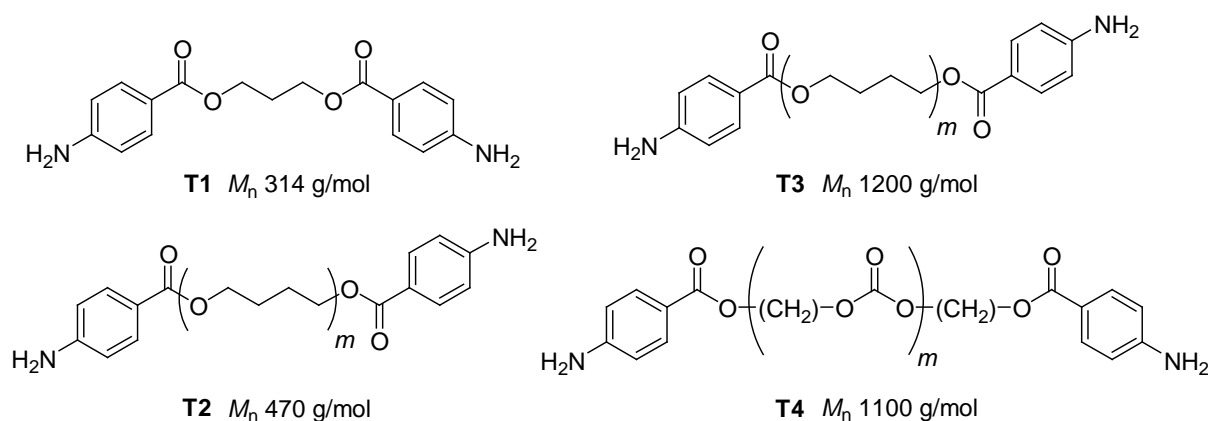
Scheme 3. Schematic representation of a segmented polymer chain (a) without and (b) with the use of a chain extender illustrating the increase in hard segment content as a result of a copolymerization with a short-chain telechelic.
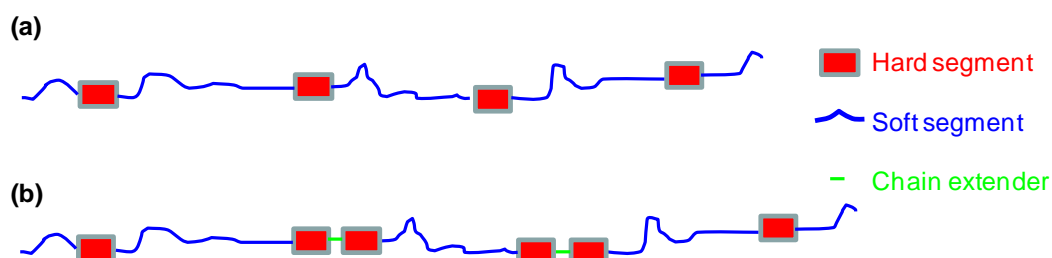
Table 1. Details of polymer composition, molar mass averages, thermal transitions and breaking strain.

| Polymer	Composition	M_n (g mol^{-1})	M_w/M_n	T_g (°C)	T_{ms} (°C)	T_{flow} (°C)	%Strain at break
P1	PCL4200	85,000	1.41	–53	53	76 [a]	630
P2	PCL4200:T1 (2:1)	110,000	1.84	–52	46	179	850
P3	PCL4200:T1 (5:1)	74,000	1.95	–55	47	66	640
P4	PCL4200:T2 (2:1)	63,000	1.54	–52	52	n.d. [b]	8
P5	PCL4200:T2 (5:1)	85,000	1.39	–58	46	n.d.	640
P6	PCL4200:T3 (2:1)	100,000	1.36	–58	47	120	240
P7	PCL4200:T3 (5:1)	135,000	1.37	–59	45	107	620
P8	PCL4200:T4 (2:1)	170,000	1.41	–59	49	96	Brittle
P9	PCL4200:T4 (5:1)	234,000	1.41	–57	50	83	n.d.
P10	PCL8200	170,000	1.41	–57	57	~60	890
P11	PCL8200:T1 (1:1)	110,000	1.34	–57	55	n.d.	1,320
P12	PCL8200:T1 (1:2)	n.d.	n.d.	–55	50	>150	695
P13	PCL8200:T3 (1:1)	150,000	1.47	–57	52	130	1,030
P14	PCL8200:T3 (1:2)	85,000	1.37	–58	53	124	785
P15	PCL8200:T3 (1:3)	110,000	1.55	–60	52	127	Brittle
P16	PCL8200:T3 (1:4)	90,000	1.68	–60	54	147	510
P17	PCL8200:T3 (1:5)	70,000	1.60	n.d.	53	153	Brittle
P18	PCL8200:T4 (1:4)	110,000	1.35	–48	48	>150	1,540

[a] Melting transition detected by DSC. [b] Not determined.

2.2. Gel-Permeation Chromatography

Number-average molar masses, M_n, were determined by gel-permeation chromatography (GPC) and ranged from 63 to 234 kg mol^{-1} (Table 1). Polymer formation was also evident from an increase in viscosity during the synthesis. The polydispersity index, M_w/M_n, was found to be between 1.4 and 1.7 which is typical for a step-growth polymerization after precipitation of the polymer during work-up.

## 2.3. Differential Scanning Calorimetry

Differential scanning calorimetry (DSC) revealed a glass transition for all polymers at about –55 °C which could be attributed to the PCL soft segment, the major component of the segmented copolymers (Table 1). The melting temperature of the soft segments (T_{ms}) was evident as a large endothermic peak at 45–52 °C for polymers made with **PCL4200**, and at 48–57 °C for polymers containing **PCL8200** as the main soft segment. These values approached the melting temperature for high-molecular-weight polycaprolactone (60 °C). Only **P1**, a homopolymer, gave rise to a small endothermic peak at 76 °C indicative of the melting of the aramid hard segment. For none of the other polymers was it possible to detect a similar melting endotherm for the hard segment by DSC. The most likely reasons were the relatively small amount of hard segment present together with an increased mixing of hard and soft segment phases resulting from an irregular copolymer structure.

Figure 1. DSC curves for selected SMPs.
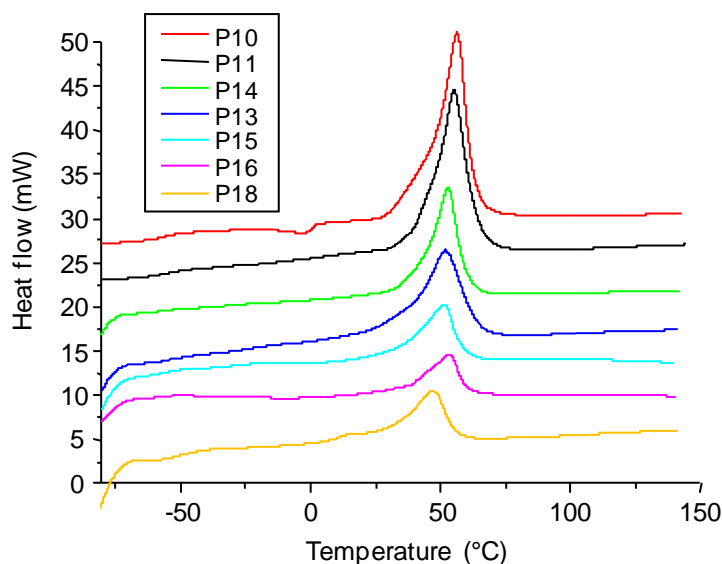
2.4. Tensile Tests

The incorporation of polycaprolactone soft segments was not expected to give an elastic material since PCL (the major component of the soft segments) is semicrystalline at room temperature. Stress–strain curves were therefore characteristic for flexible plastics. A typical stress–strain curve is shown in Figure 2. The Young's modulus was calculated from the initial slope and its values ranged from 70 to 200 MPa. All polymers showed evidence of a yield point and neck formation which was followed by a more gentle rise in stress as the amorphous chains crystallized before the samples finally broke.

Table 1 summarizes breaking strains. We note that films of **P4** and **P6** showed very low elongations at break, whereas several other polymers were too brittle for tensile tests. This was attributed to either a low molecular weight or poor film-forming properties. Only polymers with a breaking strain exceeding 600% were considered suitable for further investigation.

Figure 2. Stress–strain curve for polymer **P14**.
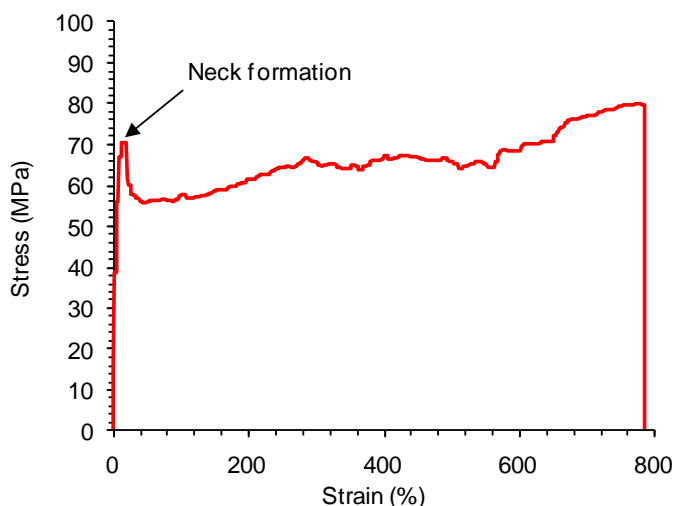
2.5. Dynamic Mechanical Thermal Analysis

Dynamic mechanical analysis served as a key characterization technique for screening the series of (co)polymers for potential shape-memory properties [13]. We will first discuss the data for polymers containing the shorter polycaprolactone **PCL4200** soft segments.

Figure 3a shows the temperature-dependence of the storage modulus of **P2**–**P9**. In all cases, the storage modulus decreased steadily above –60 °C, the T_g of the soft segment. An additional drop in storage modulus was observed at around T_{ms}.

For optimum performance, the drop in modulus for a shape-memory polymer should not only be large and sharp, it should ideally be followed by an extended rubbery plateau. The DMTA measurement helped not only in determining the presence of a rubbery plateau but also in identifying an upper service temperature. The flow temperature, T_{flow}, was estimated as the temperature at which the storage modulus fell below 1 MPa (Table 1). While all polymers showed the desired steep decline in modulus at around 50 °C, few had a flow temperature above 100 °C. Increasing length and amount of the soft segment noticeably lowered T_{flow} which was ~70 °C for the **PCL4200**-based homopolymer **P1** whereas for the **PCL8200**-based **P10** (54 °C) it more or less coincided with the melting of the soft segments. This observation was not surprising and confirmed Kim *et al*. who noted that the increase in soft segment content drastically lowers the rubbery modulus [7]. As a consequence of the low flow temperature and a virtually non-existent rubbery plateau, polymers **P1** and **P10** deformed irreversibly upon heating above T_{ms}, and neither homopolymer exhibited a shape-memory effect.

The incorporation of a chain extender (**T1**–**T4**) was expected to increase both the hard segment and the flow temperature of the polymers, and this was indeed the case (Table 1). The rubbery plateau widened and, not surprisingly, the rubbery modulus increased as well, particularly with the short-chain **T1** as the chain extender. The latter was also the most effective in raising the flow temperature again well above T_{ms}. A flow temperature above 100 °C was considered sufficient to avoid irreversible deformation upon heating to slightly above T_{ms}, a key feature of the shape-memory test cycle (see Section 2.6). Three copolymers (**P2**, **P6** and **P7**) in the first series fulfilled this criterium.

Figure 3. Plot of (a) the storage modulus and (b) tan δ as a function of temperature for polymers **P2**–**P9**.
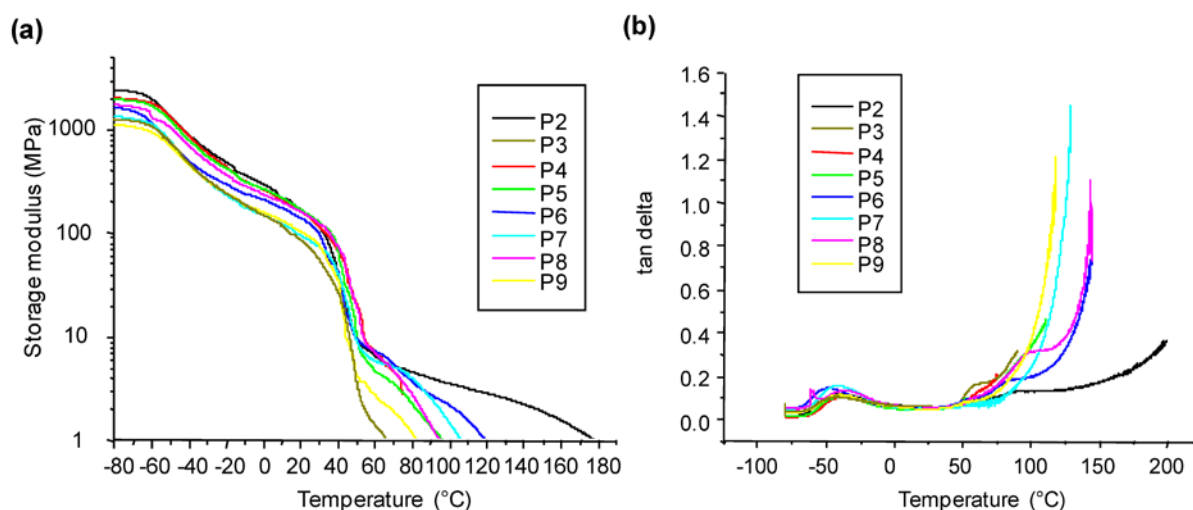
Tan delta, the ratio of loss modulus (not shown) to storage modulus, provides an indication of how easily elastic energy is stored, or lost in the form of heat, during a stretch–relaxation cycle as occurs in a DMTA experiment or a cyclic tensile test (the standard test for shape-memory polymers). A good elastomer should possess a tan δ well below 0.1, whereas a tan $\delta > 0.5$ is likely to lead to significant losses of elastic energy in form of heat (*i.e.*, damping). Figure 3b shows a plot of tan δ as a function of temperature for **P2**–**P9**. A maximum is observed around the glass transition. Most polymers in this series exhibited a steep rise in tan δ above 50 °C, that is, at about T_{ms}. Only **P2** and **P6** had tan δ values below 0.1 up to 80 °C. All remaining polymers were prone to a high damping behavior already at 60 °C, the temperature chosen for the shape recovery experiments in the subsequent cyclic tensile tests.

Figure 4. Plot of (a) the storage modulus and (b) tan δ as a function of temperature for polymers **P10**–**P16**. Arrows indicate the onset of irreversible sample deformation.
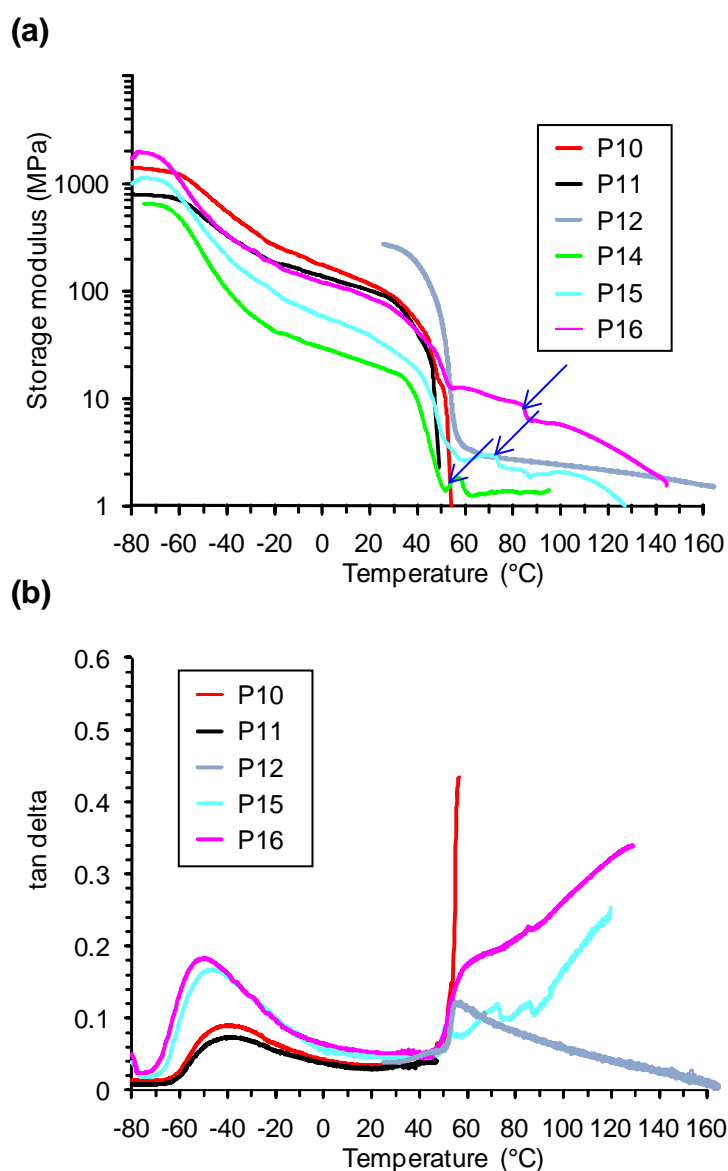
Understanding the dependence of the shape-memory properties to the tan delta curve would make future work easier because unsuitable polymers could be sorted out prior to the time-consuming cyclic

measurements. Figure 4 shows the temperature-dependence of the storage modulus of the polymers containing the longer polycaprolactone **PCL8200** soft segment. In all cases, the storage modulus displayed a significant drop at T_{ms}, as desired for an SMP. DMTA measurements also revealed irregularities in the modulus *vs.* temperature plots such as a step or slip, which coincided with irreversible sample deformation, for all polymers except **P12** and **P16**. Several polymers did not show any rubbery plateau at all.

2.6. Cyclic Thermomechanical Tests

Polymers **P2**, **P6**, **P7**, **P11**, **P12**, **P16** and **P18** were selected for cyclic stress–strain tests because (i) their storage modulus *vs.* temperature curves showed the required extended rubbery plateau and (ii) tan delta was in most cases still comparatively low and indicated elastic behavior. Samples of these polymers were elongated to a strain of 300% at room temperature (cold drawing) and then heated to 60 °C (*i.e.*, slightly above T_{ms}) to initiate shape recovery.

Figure 5 shows the results of such cyclic tests. The first two cycles deviated most from each other. During the first cycle, the polymer chains were forced to partially disentangle within the material and, as in Figure 2, the stress–strain curve looked more like that of a thermoplastic. After having been through one cycle, all polymers adopted the typical S-shaped stress–strain curve characteristic for an elastic material. The reproducibility of the test cycle is quantitatively expressed by the strain recovery rate (Table 2). It took at least 3 cycles to achieve a steady recovery rate that remained more or less unchanged for subsequent cycles. From that point on, reproducibility was generally quite good except for **P12** where we suspected that the amount of hard segment was above its optimum. Among the other **PCL8200**-containing polymers, **P11** and **P18** recovered to 99% already after 3 cycles whereas **P16** required five cycles until the shapes of the curves almost matched each other.

Strain fixity provides information about the stability of the temporary shape. Ideally, strain fixity would be 100%, and lower values indicate that a sample relaxes to some extent after drawing even without being triggered by heat to do so. This is not uncommon during cold drawing, but can be overcome by drawing at higher temperature together with immediate freezing of the temporary shape in a cooling bath. We have opted for a cold-drawing procedure in our experiments as it avoids an extra step and is also more representative for practical applications. **P2**, **P6**, **P7** and **P16** were the polymers with the highest strain fixity rates of ≥80% (Table 2). It is interesting to note that the inclusion of a comparatively long chain extender based on a polytetrahydrofuran (**P6**, **P7**, **P16**) or polycarbonate (**P18**) was not detrimental to the shape-memory properties as might have been anticipated. **P16** was the most flexible of the shape-memory polymers which could be attributed to the incorporation of the flexible polytetrahydrofuran segments which provided some elastic properties leading to recovery of deformations already at room temperature. We also note that SMPs containing **PCL8200**-based soft segments showed poor reproducibility in the cyclic tests even with increasing numbers of cycles which we attribute to loss of elastic energy in form of heat (Figure 5e,f). It confirmed our previous observation that tan delta was high and rising above T_{ms} for these polymers.

To provide additional comparison with the literature, we performed a full shape-memory cycle for a selected sample which involved heating above T_{ms}, deformation above T_{ms}, cooling, storage in the

deformed state, then reheating to trigger shape recovery. Only polymer **P2** could be investigated in this way as most other polymers, particularly those containing **PCL8200** soft segments, could not sustain large forces at elevated temperature (60 °C) and were prone to break or deform irreversibly. This is not unexpected given the large tan delta values for these polymers at temperatures exceeding 50 °C. An additional difficulty arose due to stress in the deformed sample decreasing notably with time at 60 °C, which resulted in an artificial improvement in ε_u the longer one waited. To minimise this effect in the cyclic experiment, the cooling process was limited to 15 minutes.

Figure 5. Cyclic tensile tests for polymer (a) **P2**, (b) **P6**, (c) **P7**, (d) **P11**, (e) **P16** and (f) **P18**.
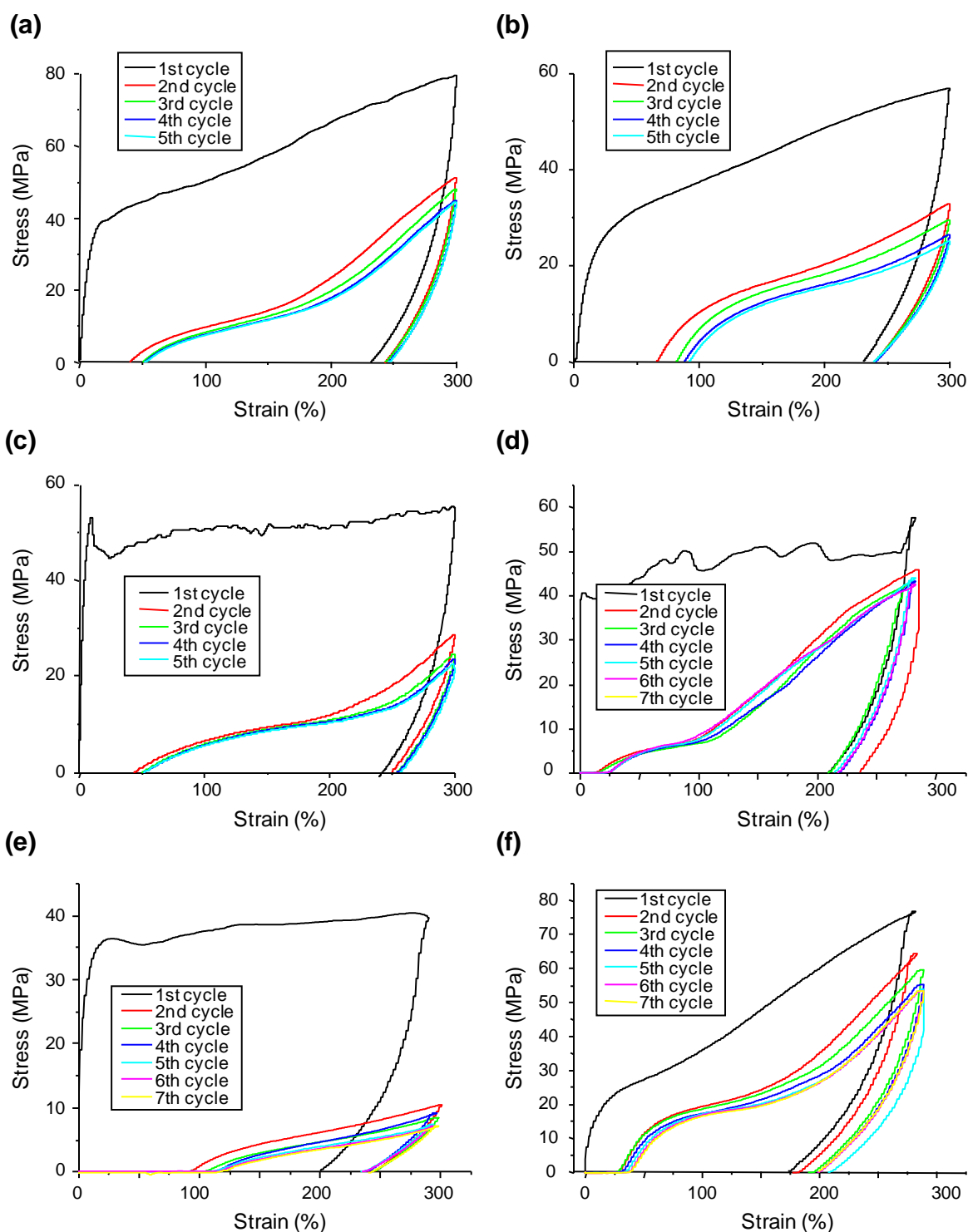
Table 2. Shape recovery rate and strain fixity during the first five thermomechanical cycles (N = number of cycle) for selected polymers.

| N	Shape recovery rate (%)							Strain fixity (%)						
	P2	**P6**	**P7**	**P11**	**P12**	**P16**	**P18**	**P2**	**P6**	**P7**	**P11**	**P12**	**P16**	**P18**
1	-	-	-	-	-	-	-	77.1	76.6	79.2	73.7	84.6	69.0	61.7
2	86.7	77.9	85.5	95.5	85.5	68.5	90.0	80.5	79.6	82.8	82.5	80.9	81.8	64.7
3	96.0	93.6	97.3	99.1	91.5	93.5	100	81.3	79.6	83.1	75.6	82.7	82.2	66.1
4	99.9	97.1	99.7	97.3	100	94.9	98.8	81.7	79.5	83.1	76.9	84.6	80.6	69.0
5	99.2	98.0	100	100	95.8	99.7	98.8	81.7	79.8	85.1	76.0	78.6	80.8	72.3

Figure 6 shows the cyclic stress–strain behaviour of polymer **P2** when a sample was stretched at 60 °C. The result is very similar to Figure 5a. Since loading at 60 °C includes a break when relaxation takes place, improved reproducibility of ε_u led to an increase in the strain fixity rate to above 86%, about 5% higher than for loading at room temperature (Table 1). Rabani[13] and Kim[7] showed previously that a reduction in the strain value from 300% to 200% also raises the strain fixity rate. From these initial results we conclude that, if it is possible to deform the sample at room temperature, it may be a better way to obtain compareable and more representative values for the shape memory properties of a polymer.

Figure 6. Cyclic stress-strain behaviour of **P2** when the sample was deformed at 60 °C.
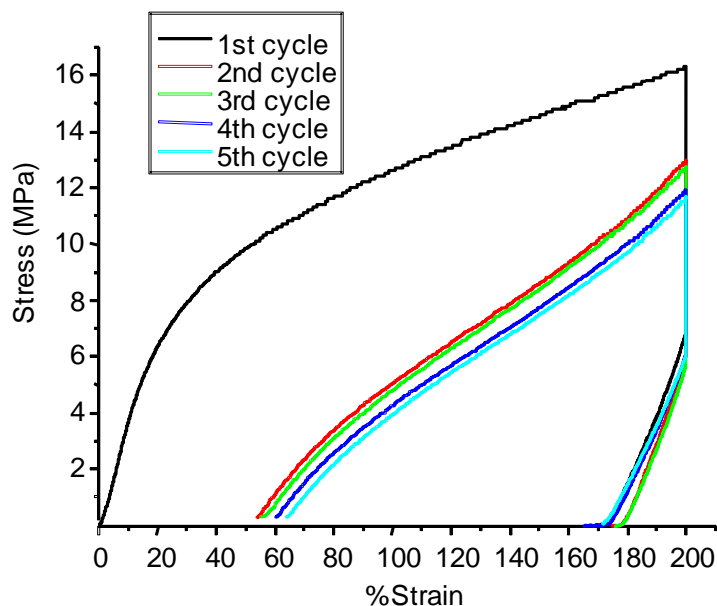
To confirm their suitability as shape-memory polymers, samples were finally tested manually. Films of these polymers could easily be drawn by hand at room temperature which resulted in the temporary (deformed) shape. The samples subsequently recovered their original shape immediately after they were warmed to 60 °C (Figure 7).

Figure 7. (a)–(c) A thin strip of shape-memory polymer **P11** was stretched at ambient temperature to several times its original length. (d)–(f) Immersion of the stretched film in a warm water bath (kept at 60 °C) resulted in the film recovering its original length.
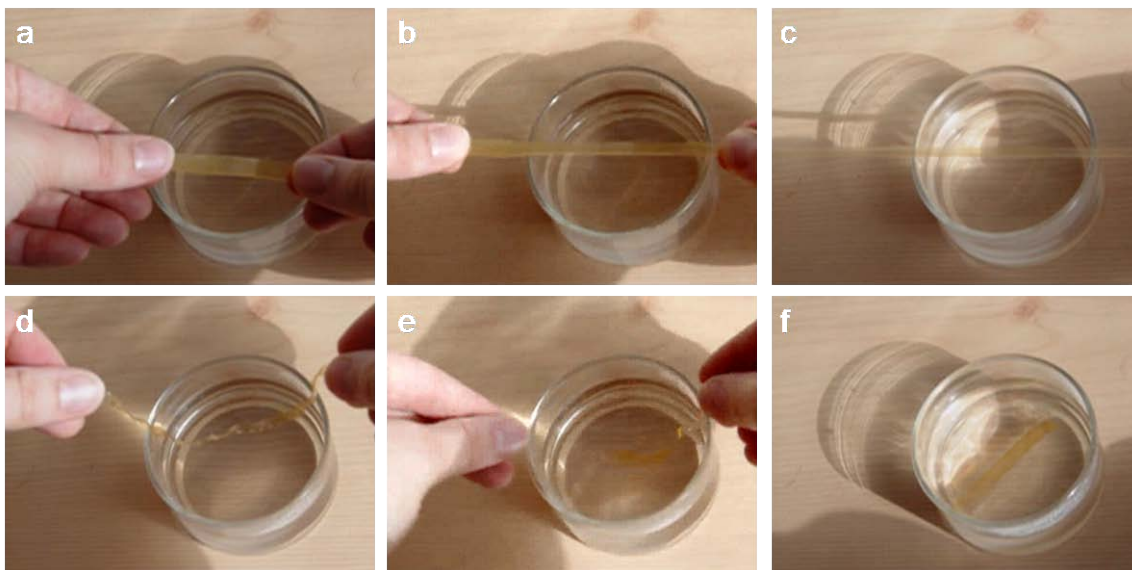
3. Experimental Section

3.1. Materials

Polycaprolactones were a gift from Solvay Polycaprolactones. Other telechelics and anhydrous *N,N*-dimethylacetamide (DMAc) were purchased from Aldrich; terephthaloyl chloride and chloro-trimethylsilane were supplied by Lancaster. The synthesis of the modified polycaprolactones **PCL4200**, **PCL8200** and telechelics **T1**–**T4** was adapted from a literature procedure and involved esterification of the telechelic diols with 4-nitrobenzoyl chloride followed by reduction with iron [11-13,16].

3.2. Typical Polymerization Procedure

PCL4200 (2.12 g, 0.50 mmol) and **T1** (78.6 mg, 0.25 mmol) were weighed into a 25 mL round-bottomed flask and dissolved in dry DMAc (10 mL) at 50 °C under nitrogen and sealed with a septum cap. After cooling the solution with an ice–water bath, chlorotrimethylsilane (0.29 mL, 2.25 mmol) was added to the stirred viscous solution with a gastight syringe and the mixture was stirred for 20 min. The polymerization was started by adding a solution of terephthaloyl chloride (152 mg, 0.75 mmol) in dry DMAc (2 mL) with a gastight syringe. The ice–water bath was removed and the solution was stirred overnight [17]. The highly viscous solution was diluted with DMAc (12 mL) and precipitated into methanol (400 mL). **P1** was obtained as a colorless rubbery polymer, collected by suction filtration, and thoroughly dried in vacuum (100 °C/0.2 mbar) until DMAc could no longer be detected in the ^{1}H NMR spectrum. Yield: 94%. IR (cm^{-1}): v 3,314 (NH str), 2,944, 2,865 (CH str), 1,725 (ester C=O str).

3.3. Characterization

^{1}H NMR spectra were recorded on a Bruker AC200 or DPX400 in $CDCl_3$. Infrared spectra were recorded on a Perkin Elmer Spectrum RX FT-IR. Molecular weight averages were determined by GPC using a Waters 590 HPLC pump and a Waters 410 differential refractometer. The GPC columns (Polymer Laboratories 5 μm mixed-C columns) were calibrated with polystyrene standards using THF as elution solvent at a flow rate of 1.0 mL min^{-1}. DSC measurements were carried out with a Thermal Advantage DSC 2010 at a heating rate of 20 °C min^{-1} under a constant nitrogen flow. Glass transitions were taken as the mid-point of the inflexion. Dynamic mechanical analysis measurements were carried out in tensile mode with a TA Instruments DMA 2980 at a frequency of 3 Hz and a heating rate of 2 °C min^{-1}. Samples were prepared by casting a viscous solution of the polymer (*ca.* 0.3–0.4 g) in DMAc (4 mL) onto Teflon plates, followed by slow evaporation of the solvent in an oven at 80 °C for 2 days. ^{1}H NMR spectra confirmed that the as-prepared polymer films no longer contained DMAc. Tensile and cyclic thermomechanical tests were carried out with cast films (cut with a razor blade to a typical size of 7 mm × 50 mm × 0.3 mm) using an Instron model 1026 tensile tester.

3.4. Cyclic Thermomechanical Tests

For work at elevated temperature, a plastic heating chamber was attached to the Instron tensile tester. The samples were heated using a heat gun at low setting, and temperature control was achieved with two thermometers. The temperature difference between both thermometers was typically around 1 °C, and the temperature could be kept constant within ±0.5 °C. For cooling to room temperature, the heat chamber was opened for 15 min.

Figure 8. Schematic stress–strain cycle: 1—stretching to ε_m; 2—stop stretching at ε_m = 300% elongation; 3—stress is removed and sample contracts to ε_u; 4—sample recovers and reaches ε_p after heating; 5—start of the next cycle.
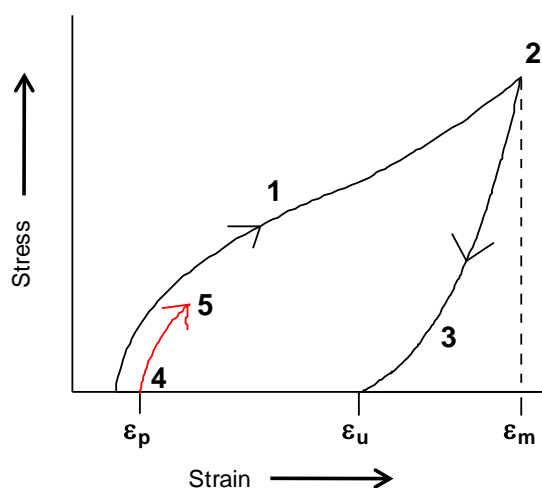
A typical sample for cyclic tests was 5 mm wide, 50 mm long and 0.4 mm thick and was elongated to a constant strain (ε_m = 300%) at 50 mm min^{-1}. The force was removed, and the sample was allowed

to relax freely at room temperature (19 °C) to reach strain ε_u (Figure 8). The sample was then heated to 60 °C for 5 min during which time it recovered. After another 15 min at room temperature, the residual strain ε_p was recorded which completed one full test cycle. The test cycle was repeated 4–6 times.

The values obtained for ε_u and ε_p were used to calculate the strain recovery rate, the total strain recovery rate, and the strain fixity rate of the shape-memory polymer [1].

Equation (1) defines the strain recovery rate and measures how much of the strain, which has been applied to the polymer, is recovered upon heating above T_{ms} from one cycle to the next (N = number of cycles).

$$\text{Strain recovery rate} = \frac{\varepsilon_m - \varepsilon_p(N)}{\varepsilon_m - \varepsilon_p(N-1)} \times 100\% \tag{1}$$

Equation (2) calculates the total strain recovery rate which expresses the change in the permanent shape after N cycles.

$$\text{Total strain recovery rate} = \frac{\varepsilon_m - \varepsilon_p(N)}{\varepsilon_m} \times 100\% \tag{2}$$

The strain fixity rate, defined by Equation (3), quantifies the ability of the crystalline soft segment to fix the deformed shape after the sample has been stretched.

$$\text{Strain fixity rate} = \frac{\varepsilon_u(N)}{\varepsilon_m} \times 100\% \tag{3}$$

For loading at 60 °C, thermostatting the chamber to 60 °C took approx. 30 minutes. The polymer film was then stretched to 200% at a rate of 10 mm min^{-1}, followed by an isothermal of 10 minutes. During this time the temperature was kept at 60 ± 0.5 °C. For cooling to room temperature, the heat chamber was opened for 15 minutes, then the sample was allowed to relax to reach ε_u.

4. Conclusions

The use of extended polycaprolactone soft segments in a segmented aramid polymer made it necessary to incorporate a short-chain telechelic (**T1** proved to be the most successful) as chain extender to further increase the hard segment component. This became particularly important for high-molecular-weight soft segment **PCL8200**.

Dynamic mechanical thermal analysis served as a useful technique to establish which polymers were suitable or unsuitable for shape-memory applications. Extended soft segments led to a large drop in modulus at around the melting temperature of the soft segment, T_{ms}. Optimum shape-memory performance required the existence of a rubbery plateau above T_{ms} and thus an optimal ratio of hard and soft segment. While **PCL8200** soft segments increased the switching temperature to around 55 °C, they also reduced the flow temperature and narrowed the rubbery plateau which was easily recognised in the storage modulus *vs.* temperature plots. Both effects were detrimental to shape-memory performance since they ultimately caused irreversible changes in dimensions of a sample film. On the other hand, large amounts of hard segment widened the rubbery plateau and made the polymers stiffer.

A sufficiently high flow temperature was equally important for applications as it provided a safety margin that ensured that the shape-memory polymer did not deform irreversibly when heated to recover its permanent shape. The most successful supplementary hard segment was **T1** which gave polymers with a flow temperature of up to 180 °C.

Polymers with excellent shape-memory properties (**P2**, **P6**) had tan delta values below 0.1 up to 80 °C, whereas many of the polymers unsuitable for shape-memory applications were prone to damping already at 60 °C, the temperature chosen for most recovery experiments. Each successful shape-memory polymer still had to undergo two or more initial "training" cycles before a reproducible performance was observed in the cyclic shape-memory tests.

Future work will have to look at the optimization of the hard segment content, as well as the best choice of chain extender. Further improvement could also be achieved by replacing terephthaloyl chloride by 2,6-naphthalenedicarbonyl dichloride, which might offer to improve the phase separation between hard and soft segment due to the stronger hydrogen bonding in substituted naphthalenedicarboxyamides [13].

Acknowledgements

References and Notes

1. Lendlein, A.; Kelch, S. Shape-memory polymers. *Angew. Chem. Int. Ed.* **2002**, *41*, 2034–2057.
2. Liu, C.; Qin, H.; Mather, P.T. Review of progress in shape-memory polymers. *J. Mater. Chem.* **2007**, *17*, 1543–1558.
3. Mohr, R.; Kratz, K.; Weigel, T.; Lucka-Gabor, M.; Moneke, M.; Lendlein, A. Initiation of shape-memory effect by inductive heating of magnetic nanoparticles in thermoplastic polymers. *Proc. Natl. Acad. Sci. USA* **2006**, *103*, 3540–3545.
4. Lendlein, A.; Jiang, H.; Jünger, O.; Kelch, S. Light-induced shape-memory polymers. *Nature* **2005**, *434*, 879–882.
5. Chung, T.; Romo-Uribe, A.; Mather, P.T. Two-way reversible shape memory in a semicrystalline network. *Macromolecules* **2008**, *41*, 184–192.
6. Bellin, I.; Kelch, S.; Langer, R.; Lendlein, A. Polymeric triple-shape materials. *Proc. Natl. Acad. Sci. USA* **2006**, *103*, 18043–18047.
7. Kim, B.K.; Lee, S.Y.; Xu, M. Polyurethanes having shape memory effects. *Polymer* **1996**, *37*, 5781–5793.
8. Lendlein, A.; Langer, R. Biodegradable, elastic shape-memory polymers for potential biomedical applications. *Science* **2002**, *296*, 1673–1676.
9. Niesten, M.C.E.J.; Feijen, J.; Gaymans, R.J. Synthesis and properties of segmented copolymers having aramid units of uniform length. *Polymer* **2000**, *41*, 8487–8500.

10. Niesten, M.C.E.J.; Ten Brinke, J.W.; Gaymans, R.J. Segmented copolyetheresteraramids with extended poly(tetramethyleneoxide) segments. *Polymer* **2001**, *42*, 1461–1469.

11. Rabani, G.; Rosair, G.M.; Kraft, A. Low-temperature route to thermoplastic polyamide elastomers. *J. Polym. Sci., Polym. Chem.* **2004**, *42*, 1449–1460.

12. Rabani, G.; Luftmann, H.; Kraft, A. Synthesis and properties of segmented copolymers containing short aramid hard segments and aliphatic polyester or polycarbonate soft segments. *Polymer* **2005**, *46*, 27–35.

13. Rabani, G.; Luftmann, H.; Kraft, A. Synthesis and characterization of two shape-memory polymers containing short aramid hard segments and poly(3-caprolactone) soft segments. *Polymer* **2006**, *47*, 4251–4260.

14. Oishi, Y.; Kakimoto, M.; Imai, Y. Synthesis of aromatic polyamides from *N,N'*-bis(trimethylsilyl)-substituted aromatic diamines and aromatic diacid chlorides. *Macromolecules* **1988**, *21*, 547–550.

15. Lozano, A.E.; de Abajo, J.; de la Campa, J.G. Synthesis of aromatic polyisophthalamides by *in situ* silylation of aromatic diamines. *Macromolecules* **1997**, *30*, 2507–2508.

16. Kato, K.; Oyaizu, Y. (Ihara Chemical Industry Co. Ltd.). Polyurethaneurea elastomer. US Patent 5,410,009, 1995.

17. In some cases the viscosity increased within the first 15 min so that the polymerization was terminated after one hour.

Electronic Supplementary Information:

Video sequence showing how shape-memory polymer **P11** is stretched by hand and recovers its original shape upon immersion in a warm water bath.